Available online at www.sciencedirect.com
SCIENCE DIRECT®
International Journal of Thermal Sciences 43 (2004) 1047–1056
International Journal of Thermal Sciences
www.elsevier.com/locate/ijts

Numerical modeling of turbulent flow in a composite porous/fluid duct utilizing a two-layer k–ε model to account for interface roughness

A.V. Kuznetsov

Department of Mechanical and Aerospace Engineering, North Carolina State University, Campus Box 7910, Raleigh, NC 27695-7910, USA

Received 22 October 2003; received in revised form 24 February 2004; accepted 25 February 2004

Available online 21 April 2004

Abstract

This paper is aimed at investigating the effect of roughness of the porous/fluid interface on turbulent convection heat transfer in composite porous/fluid ducts. It is expected that in many cases the effect of interface roughness on convection may be more significant than the effect of possible flow turbulization in the porous region. The analysis of appropriate dimensionless parameters shows that in many practical situations even if the flow in the clear fluid region is turbulent, the flow in the porous region remains laminar. The problem is thus reduced to matching the turbulent flow solution in the clear fluid region with the laminar flow solution in the porous region at the rough interface. It is shown that roughness of the porous/fluid interface significantly impacts turbulent flow in the clear fluid region as well as overall heat transfer in the duct.

1. Introduction

In recent years, there has been a renewed interest in turbulent flows in porous media as well as in composite porous/fluid domains. Antohe and Lage [1] and Getachew et al. [2] derived a κ–ε model for simulation of a macroscopic turbulence in porous media. Chung et al. [3] presented computational results obtained using the κ–ε model suggested in Refs. [1,2]. De Lemos and Pedras [4] and Pedras and de Lemos [5–8] discussed different aspects of macroscopic modeling of turbulence in homogeneous porous media. In [4], four major classes of turbulence models were identified, and the time–space and space-time averaging procedures aimed at obtaining the turbulent kinetic energy equation were compared. Masuoka et al. [9] presented an experimental study of chaotic behavior of a flow through porous media composed of a bank of tubes in a narrow gap during the transition to turbulence. Barr [10] proposed a procedure for testing the occurrence of turbulence in porous media and calculating the effective permeability when it occurs. A one-equation model for two-dimensional turbulent flow through porous media is suggested in Alvarez et al. [11]. This model is based on the assumption that the production term in the turbulent kinetic energy transport equation is proportional to the cube of velocity. Semi-empirical modeling of flow and heat transfer in porous media is considered in Flick et al. [12]. A weak turbulence regime that may occur in a porous layer heated from below is discussed in Vadasz [13]. A good review of some early turbulence models is presented in Lage [14].

There is also considerable interest in turbulent flows in composite porous/fluid domains. Hahn et al. [15] reported the results of direct numerical simulation of turbulent flow in composite porous/fluid ducts. Prakash et al. [16,17] investigated turbulent flow generated by a round water jet that impinges on porous foam. Silva and de Lemos [18] and de Lemos and Silva [19] developed a model for a turbulent flow in a composite porous/fluid domain that accounts for the turbulence generated by the porous matrix. Kuznetsov and Xiong [20] suggested that the flow in composite porous/fluid domains can be modeled by assuming turbulent flow in the clear (of solid obstacles) fluid region and laminar flow in the porous region. They emphasized that even though the flow in the porous region is assumed laminar, it is important to use the Forchheimer correction in the momentum equation and thermal dispersion term in the energy equation for the porous region. It should be noted that there is a difference in opinions about the physical origin of the Forchheimer drag and thermal dispersion. Masuka and Takatsu [21] suggested that the Forchheimer flow resistance and thermal dispersion are caused mainly by turbulent mixing in porous media. A different point of view is shared by Nield [22] who, referencing

E-mail address: avkuznet@eos.ncsu.edu (A.V. Kuznetsov).

1290-0729/$ – see front matter
doi:10.1016/j.ijthermalsci.2004.02.011

Nomenclature

a_f	fluid thermal diffusivity ..... $m^2 \cdot s^{-1}$
a_T	eddy diffusivity of heat ..... $m^2 \cdot s^{-1}$
A_ε	closure coefficient for k–l model, $= 5.0$
A_ν^0	closure coefficient for k–l model, $= 62.5$
A_ν	closure coefficient for k–l model, $\max[1, A_\nu^0(1 - k_s^+/90)]$
c_F	Forchheimer coefficient
C	dimensionless experimental constant in the correlation for thermal dispersion
C_l	closure coefficient for k–l model, $= 2.5$
$C_{\varepsilon 1}$	closure coefficient for k–ε model, $= 1.44$
$C_{\varepsilon 2}$	closure coefficient for k–ε model, $= 1.92$
C_μ	closure coefficient for k–ε model, $= 0.09$
d_p	average diameter of a porous particle ..... m
Da	Darcy number, K/R^2
h	heat transfer coefficient ..... $W \cdot m^{-2} \cdot K^{-1}$
k	turbulence kinetic energy ..... $m^2 \cdot s^{-2}$
k^+	dimensionless turbulence kinetic energy, k/u_τ^2
k_f	fluid thermal conductivity ..... $W \cdot m^{-1} \cdot K^{-1}$
k_m	stagnant thermal conductivity of the porous medium ..... $W \cdot m^{-1} \cdot K^{-1}$
k_s	equivalent sand-grain roughness ..... m
k_s^+	dimensionless equivalent sand-grain roughness, $k_s u_\tau / \nu_f$
K	permeability of the porous region ..... m^2
l_ε^+	dimensionless turbulence lenghthscale, defined by Eq. (11)
l_ν^+	dimensionless turbulence lenghthscale, defined by Eq. (12)
Nu	Nusselt number, $h2R/k_f$
p	pressure ..... Pa
Pr	Prandtl number, ν_f/a_f
Pr_t	turbulent Prandtl number, ν_T/a_T
q''_W	wall heat flux ..... $W \cdot m^{-2}$
r	radial coordinate ..... m
r^+	dimensionless radial coordinate, $u_\tau r/\nu_f$
R	duct radius ..... m
R^+	dimensionless duct radius, $u_\tau R/\nu_f$
Re_K	Reynolds number based on filtration velocity in the bulk of the porous region and $K^{1/2}$ as characteristic length, defined by Eq. (49)
Re_p	Reynolds number based on the average particle diameter and the friction velocity at the porous/fluid interface, $u_\tau d_p/\nu_f$
R_y	interface-distance Reynolds number, $y_{\text{eff}} k^{1/2}/\nu_f$
$Re_{2\xi R}$	Reynolds number based on the width of the clear fluid region and the mean velocity in this region, defined by Eq. (47)
T	temperature ..... K
T_m	mean flow temperature ..... K
T_W	wall temperature ..... K
u	longitudinal velocity, ... $m \cdot s^{-1}$
u^+	dimensionless velocity, u/u_τ
u_i^+	dimensionless filtration velocity at the porous/fluid interface
u_τ	friction velocity at the porous/fluid interface, $(\tau_i/\rho_f)^{1/2}$ ..... $m \cdot s^{-1}$
U_m^+	dimensionless mean flow velocity in the duct, defined by Eq. (25)
y^+	dimensionless distance from the porous/fluid interface, $\xi R^+ - r^+$
y_{eff}^+	modified dimensionless distance from the porous/fluid interface, $y^+ + y_0^+$
y_{match}^+	matching point of k–l and k–ε models, defined by Eq. (20)
y_0^+	dimensionless hydrodynamic roughness

Greek symbols

β	dimensionless adjustable coefficient in the matching condition for the shear stress at the porous/fluid interface
ε	turbulence dissipation rate ..... $m^2 \cdot s^{-3}$
ε^+	dimensionless turbulence dissipation rate, $\varepsilon \nu_f / u_\tau^4$
θ	dimensionless temperature for the uniform wall heat flux case, $(1/Nu)(T - T_W)/(T_m - T_W)$
μ_{eff}	effective viscosity of porous medium ..... $kg \cdot m^{-1} s^{-1}$
μ_f	fluid viscosity ..... $kg \cdot m^{-1} s^{-1}$
ν_f	fluid kinematic viscosity ..... $m^2 \cdot s^{-1}$
ν_T	eddy diffusivity of momentum ..... $m^2 \cdot s^{-1}$
ν_T^+	dimensionless eddy viscosity, ν_T/ν_f
ξ	dimensionless position of the interface, defined in Fig. 1
ρ_f	fluid density ..... $kg \cdot m^{-3}$
σ_ε	closure coefficient for k–ε model, $= 1.3$
τ_i	shear stress at the porous/fluid interface $N \cdot m^{-2}$
ϕ	dimensionless temperature for the uniform wall temperature case, $(T - T_W)/(T_m - T_W)$
φ	porosity

a book by Bear [23], pointed out that actual turbulence occurs at values of the Reynolds number at least one order of magnitude higher than that at which the flow starts deviating from the Darcy law. Recently, Macedo et al. [24] investigated turbulence effects on a flow through a pseudo porous medium by numerically solving a set of Reynolds-averaged Navier–Stokes equations with the κ–ε model for turbulence. A two-dimensional porous medium was obtained by randomly placing solid obstacles. A surprisingly good agreement with the Forchheimer's equation for a turbulent flow at relatively small Reynolds numbers was observed. For high Reynolds number conditions, a deviation from the results predicted by the Forchheimer equation was observed. The results of [24] thus suggest that the Forchheimer equation may be acceptable to model not only laminar flow in porous media, but also the transitional regime or maybe even weak turbulence.

In composite porous/fluid domains, most of the flow is expected to occur in the clear fluid region; therefore, in most cases the flow in the porous region either remains laminar or just starts its transition to turbulence even if the flow in the clear fluid region is fully turbulent. This conclusion is confirmed later on in the paper by comparing appropriate Reynolds numbers with their critical values. Therefore, for most cases, using the Forchheimer term in the momentum equation and the thermal dispersion term in the energy equation for the porous region may result in a sufficiently good model for the porous region. However, what may really affect turbulent convection in composite domains is the roughness of the porous/fluid interface. If particles or fibers that constitute the porous medium (and the pores) are relatively large, the impact of the roughness of the porous/fluid interface on convection heat transfer in composite porous/fluid domains may be much more significant than the impact of possible turbulence in the porous region.

The aim of this paper is to extend the approach suggested in Ref. [20] in two ways. The model presented in [20] assumed a hydraulically smooth interface. In this paper this restriction is lifted and the model is extended to the case of a rough interface. The effects of the interface roughness on turbulent forced convection in a composite porous/fluid duct are extensively studied. Secondly, the model of [20] relied on a simplified algebraic model to calculate turbulent viscosity in the clear fluid region. In this paper a much more accurate κ–ε model is utilized. To enable the utilization of the κ–ε model for the domain with a rough interface, this model is combined with a κ–l model which is used near the interface, as suggested in Durbin et al. [25] and Rodi [26]. At a matching point, which is located in the clear fluid region at some distance from the interface, computations are switched from κ–l to κ–ε model, the latter is utilized in the core of the clear fluid region.

A composite circular duct considered in this paper is displayed in Fig. 1. The central portion of the duct, $0 \leqslant r \leqslant \xi R$, is occupied by a clear fluid while the peripheral potion, $\xi R \leqslant r \leqslant R$, is occupied by an isotropic fluid-saturated porous medium of uniform porosity. The wall of the duct is subject to either uniform heat flux or uniform wall temperature.

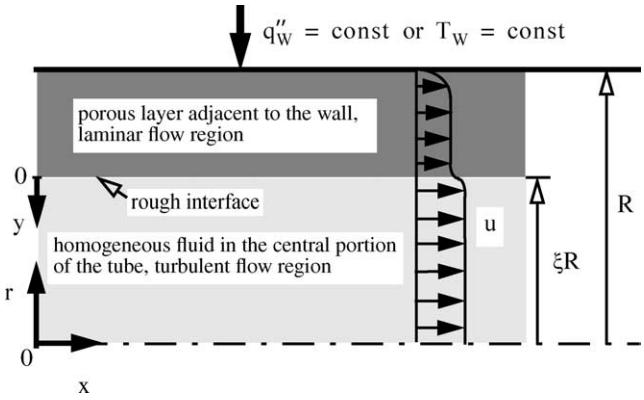

Fig. 1. Schematic diagram of the problem.

2. Mathematical model

As Fig. 1 shows, the flow domain can be divided into two regions, the central clear fluid region, where the flow is turbulent, and the peripheral porous region, where the flow is assumed to be laminar.

2.1. Momentum equation and turbulence model for the clear fluid region

For hydrodynamically fully developed flow, the velocity distribution in the clear fluid region is computed from the following equation [27]:

$$\frac{\mathrm{d}u^+}{\mathrm{d}y^+} = \frac{1}{1+\nu_T^+}\left(1-\frac{y^+}{\xi R^+}\right) \tag{1}$$

where u^+ is the dimensionless velocity, u/u_τ; u is the longitudinal velocity; u_τ is the friction velocity at the porous/fluid interface, $\sqrt{\tau_i/\rho_f}$; τ_i is the shear stress at the porous/fluid interface (at $r = \xi R$); ρ_f is the fluid density; R^+ is the dimensionless radius of the duct, $u_\tau R/\nu_f$; R is the duct radius; ν_f is the fluid kinematic viscosity; y^+ is the dimensionless distance from the porous/fluid interface towards the duct center, $\xi R^+ - r^+$; r^+ is the dimensionless radial coordinate, $u_\tau r/\nu_f$; r is the radial coordinate; ν_T^+ is the dimensionless eddy viscosity, ν_T/ν_f; ν_f is the fluid kinematic viscosity; and ν_T is the eddy diffusivity of momentum.

Durbin et al. [25] suggested utilizing a combination of k–l (in the vicinity of the wall) and k–ε (in the rest of the domain) models to account for the roughness of the wall. In this paper, this combined model is applied to the clear fluid region, $0 \leqslant r^+ \leqslant \xi R^+$. This allows accounting for the roughness of the porous/fluid interface.

In the core of the clear fluid region, when $y^+_{\mathrm{match}} \leqslant y^+ \leqslant R^+$ (the equation for the matching point is given later on),

the following k–ε model is utilized. For the fully developed flow, the turbulence kinetic energy equation can be presented as:

$$\nu_T^+\left(\frac{\partial u^+}{\partial r^+}\right)^2 - \varepsilon^+ + \frac{1}{r^+}\frac{\partial}{\partial r^+}\left[r^+\left(1+\nu_T^+\right)\frac{\partial k^+}{\partial r^+}\right] = 0 \qquad (2)$$

where

$$k^+ = k/u_\tau^2, \qquad \varepsilon^+ = \varepsilon\nu_f/u_\tau^4 \qquad (3)$$

The dissipation rate equation for the fully developed flow is

$$C_{\varepsilon 1}\frac{\varepsilon^+}{k^+}\nu_T^+\left(\frac{\partial u^+}{\partial r^+}\right)^2 - C_{\varepsilon 2}\frac{(\varepsilon^+)^2}{k^+} + \frac{1}{r^+}\frac{\partial}{\partial r^+}\left[r^+\left(1+\frac{\nu_T^+}{\sigma_\varepsilon}\right)\frac{\partial \varepsilon^+}{\partial r^+}\right] = 0 \qquad (4)$$

The dimensionless eddy viscosity can be found from the following equation:

$$\nu_T^+ = C_\mu\frac{(k^+)^2}{\varepsilon^+} \qquad (5)$$

The closure coefficients for the k–ε model are

$$C_{\varepsilon 1} = 1.44, \qquad C_{\varepsilon 2} = 1.92, \qquad \sigma_\varepsilon = 1.3, \qquad C_\mu = 0.09 \qquad (6)$$

In the vicinity of the fluid/porous interface, when $0 \leqslant y^+ \leqslant y^+_{\text{match}}$, the following k–l model is utilized. Eq. (2) stands, but instead of Eq. (4) the dissipation rate is found from the following equation:

$$\varepsilon^+ = \frac{(k^+)^{3/2}}{l_\varepsilon^+} \qquad (7)$$

where

$$l_\varepsilon^+ = l_\varepsilon\frac{u_\tau}{\nu_f} \qquad (8)$$

Instead of Eq. (5), the dimensionless eddy viscosity is found from the following equation

$$\nu_T^+ = C_\mu\left(k^+\right)^{1/2} l_\nu^+ \qquad (9)$$

where

$$l_\nu^+ = l_\nu\frac{u_\tau}{\nu_f} \qquad (10)$$

For this k–l model, the Van Driest form of length scales is adopted:

$$l_\varepsilon^+ = C_l y_{\text{eff}}^+\left(1 - e^{-R_y/A_\varepsilon}\right) \qquad (11)$$

and

$$l_\nu^+ = C_l y_{\text{eff}}^+\left(1 - e^{-R_y/A_\nu}\right) \qquad (12)$$

where

$$y_{\text{eff}}^+ = y_{\text{eff}}\frac{u_\tau}{\nu_f} \qquad (13)$$

and

$$R_y = y_{\text{eff}}k^{1/2}/\nu_f = y_{\text{eff}}^+\left(k^+\right)^{1/2} \qquad (14)$$

is the interface-distance Reynolds number. y_{eff}^+ in Eqs. (11)–(14) is the modified dimensionless distance from the interface, which accounts for the interface roughness and can be calculated as follows:

$$y_{\text{eff}}^+ = y^+ + y_0^+ \qquad (15)$$

where y_0^+ is the dimensionless hydrodynamic roughness, which can be related to the dimensionless equivalent sand-grain roughness parameter, $k_s^+ (= k_s u_\tau/\nu_f)$, by an equation given in Cebeci and Chang [28]:

$$y_0^+ = 0 \quad \text{if } k_s^+ \leqslant 4.535$$

(this corresponds to a hydraulically smooth surface) (16a)

$$y_0^+ = 0.9\left[\sqrt{k_s^+} - k_s^+\exp\left(-k_s^+/6\right)\right] \quad \text{if } k_s^+ > 4.535$$

(this corresponds to a hydraulically rough surface) (16b)

Alternatively, a calibration procedure described in Ref. [25] can be utilized to find a relation between y_0^+ and k_s^+. A dependence of y_0^+ obtained as a result of such calibration is displayed in Fig. 2 of Ref. [25]. To complete modeling the effect of interface roughness, it is necessary to relate the equivalent dimensionless sand-grain roughness parameter, k_s^+, to the Darcy number and porosity in the porous region. According to the Carman–Kozeny equation [29], the average diameter of a solid particle that constitutes the porous medium can be estimated as:

$$d_p = \frac{\sqrt{180}(1-\varphi)K^{1/2}}{\varphi^{3/2}} \qquad (17)$$

where K is the permeability and φ is the porosity.

Assuming that the equivalent sand-grain roughness parameter, k_s, can be estimated as $d_p/2$ (Prof. D.A. Nield [30] noted that this a good estimate providing the porous medium is machined to have a "plane" interface; in the case of a "coastline" $d_p/2$ gives just a lower bound on the roughness), the following equation for k_s^+ is obtained:

$$k_s^+ = \frac{u_\tau}{\nu}k_s = \frac{u_\tau}{\nu}\frac{\sqrt{180}(1-\varphi)}{2\varphi^{3/2}}K^{1/2} = R^+\frac{6.70(1-\varphi)}{\varphi^{3/2}}Da^{1/2} \qquad (18)$$

where Da is the Darcy number, K/R^2.

The closure coefficients for the k–l model are

$$C_l = 2.5, \qquad A_\varepsilon = 5.0, \qquad A_\nu^0 = 62.5,$$
$$A_\nu = \max\left[1, A_\nu^0\left(1 - k_s^+/90\right)\right] \qquad (19)$$

According to [25], the point where the k–l model (which is used near the interface) must be switched to k–ε model is found as

$$y_{\text{match}}^+ = \log(20)A_\nu/\left(k^+\right)^{1/2} \qquad (20)$$

The boundary conditions for k and ε equations are

$$k^+(0) = \frac{1}{\sqrt{C_\mu}}\min\left[1, \left(k_s^+/90\right)^2\right] \qquad (21)$$

where k_s^+ is given by Eq. (18).

In the center of the pipe because of the symmetry

$$\partial k^+/\partial r^+ = 0 \quad \text{and} \quad \partial \varepsilon^+/\partial r^+ = 0 \tag{22}$$

In the matching point defined by Eq. (20) the turbulence kinetic energy and the dissipation rate must be continuous.

2.2. Momentum equation for the porous region

The Brinkman–Forchheimer-extended Darcy equation [29] is utilized to model the assumed laminar flow in the porous region. Utilizing the dimensionless variables defined above, this equation can be presented as [20]:

$$\frac{2}{\xi R^+} + \left(\frac{\mu_{\text{eff}}}{\mu_f}\right)\frac{1}{r^+}\frac{\mathrm{d}}{\mathrm{d}r^+}\left(r^+\frac{\mathrm{d}u^+}{\mathrm{d}r^+}\right) - \frac{u^+}{Da(R^+)^2} - \frac{c_F}{Da^{1/2}R^+}\left(u^+\right)^2 = 0 \tag{23}$$

where c_F is the Forchheimer coefficient, μ_f is the fluid dynamic viscosity, and μ_{eff} is the effective dynamic viscosity in the porous region.

2.3. Energy equation for the clear fluid region

The energy equation for the clear fluid region is based on the constant turbulent Prandtl number model. More sophisticated models can be easily used with the approach developed in this paper. Since the flow is hydrodynamically and thermally fully developed, for the *uniform wall heat flux case* the energy equation can be presented as:

$$\frac{1}{r^+}\frac{\mathrm{d}}{\mathrm{d}r^+}\left[\left(1+\nu_T^+\frac{Pr}{Pr_t}\right)r^+\frac{\mathrm{d}\theta}{\mathrm{d}r^+}\right] = -\frac{1}{(R^+)^2}\frac{u^+}{U_m^+} \tag{24}$$

where Pr is the Prandtl number, ν_f/a_f; a_f is the fluid thermal diffusivity; Pr_t is the turbulent Prandtl number, ν_T/a_T; a_T is the eddy diffusivity of heat; and U_m^+ is the mean fluid velocity in the duct:

$$U_m^+ = \frac{2}{(R^+)^2}\int_0^{R^+} u^+ r^+ \,\mathrm{d}r^+ \tag{25}$$

In Eq. (24), θ is the dimensionless temperature for the *uniform heat flux case* (the dimensionless temperature for the uniform wall temperature case is defined differently):

$$\theta = (1/Nu)(T - T_W)/(T_m - T_W) \tag{26}$$

where T is the temperature, T_W is the wall temperature (at $r^+ = R^+$), T_m is the mean temperature in the duct:

$$T_m = \frac{2}{R^2 U_m}\int_0^R uTr \,\mathrm{d}r \tag{27}$$

and Nu is the Nusselt number:

$$Nu = h2R/k_f = 2Rq''/\left[k_f(T_W - T_m)\right] \tag{28}$$

where h is the heat transfer coefficient.

For the *uniform wall temperature case* the energy equation can be presented as:

$$\frac{1}{r^+}\frac{\mathrm{d}}{\mathrm{d}r^+}\left[\left(1+\mu_T^+\frac{Pr}{Pr_t}\right)r^+\frac{\mathrm{d}\phi}{\mathrm{d}r^+}\right] = -\frac{1}{(R^+)^2}Nu\,\phi\frac{u^+}{U_m^+} \tag{29}$$

where

$$\phi = (T - T_W)/(T_m - T_W) \tag{30}$$

is the dimensionless temperature for the *uniform wall temperature case.*

2.4. Energy equation for the porous region

For the *uniform wall heat flux case* the energy equation for the porous region can then be presented as:

$$\frac{1}{r^+}\frac{\mathrm{d}}{\mathrm{d}r^+}\left[\left(\frac{k_m}{k_f} + CPr\,Re_p u^+\right)r^+\frac{\mathrm{d}\theta}{\mathrm{d}r^+}\right] = -\frac{1}{(R^+)^2}\frac{u^+}{U_m^+} \tag{31}$$

where C is the dimensionless experimental constant in the correlation for thermal dispersion; k_f is the fluid thermal conductivity; k_m is the stagnant thermal conductivity of the porous medium (when $u^+ = 0$); $Re_p = u_\tau d_p/\nu_f$ is the Reynolds number based on the average particle diameter, d_p, and the friction velocity at the porous/fluid interface, u_τ.

The term $CPr\,Re_p u^+$ in Eq. (31) accounts for the transverse thermal dispersion [31–33]. Longitudinal thermal dispersion and longitudinal thermal conduction are neglected, which are valid assumptions if the Péclet number is large.

For the *uniform wall temperature case* the energy equation for the porous region is:

$$\frac{1}{r^+}\frac{\mathrm{d}}{\mathrm{d}r^+}\left[\left(\frac{k_m}{k_f} + CPr\,Re_p u^+\right)r^+\frac{\mathrm{d}\phi}{\mathrm{d}r^+}\right] = -\frac{1}{(R^+)^2}Nu\,\phi\frac{u^+}{U_m^+} \tag{32}$$

2.5. Compatibility condition

Once the velocity and temperature distributions are computed, the Nusselt number can be computed utilizing a compatibility condition [34]. For the *uniform wall heat flux case* the compatibility condition is

$$Nu = U_m^+\left(R^+\right)^2/\left[2\int_0^{R^+} u^+\theta r^+ \,\mathrm{d}r^+\right] \tag{33}$$

For the uniform wall temperature case the compatibility condition is

$$Nu = -2\frac{k_m}{k_f}R^+\frac{\mathrm{d}\phi}{\mathrm{d}r^+}\Big|_{r^+=R^+} \tag{34}$$

2.6. Boundary conditions

At the duct wall, $r^+ = R^+$, a no-slip hydrodynamic boundary condition is imposed:

$$u^+ = 0 \tag{35}$$

From the definition of the dimensionless temperatures (Eqs. (26) and (30)) it follows that at $r^+ = R^+$

$$\theta = 0 \tag{36}$$

for the *uniform wall heat flux case* and

$$\phi = 0 \tag{37}$$

for the *uniform wall temperature case*.

From the definitions of u^+ and r^+ (or simply from Eq. (1)) it follows that

$$\left.\frac{\partial u^+}{\partial r^+}\right|_{r^+=\xi R^+-0} = -\frac{1}{1+\nu_T^+|_{r^+=\xi R^+}} \tag{38}$$

It should be noted that because the interface is rough, the dimensionless eddy viscosity, ν_T^+, is not equal to zero at the interface (cf. Eqs. (21) and (9)). The jump in the shear stress condition suggested by Ochoa-Tapia and Whitaker [35,36] for modeling a porous/fluid interface can be presented as:

$$\left(\frac{\nu_{\text{eff}}}{\nu_f+\nu_T|_{r^+=\xi R^+}}\right)\left.\frac{\partial u^+}{\partial r^+}\right|_{r^+=\xi R^+ +0} - \left.\frac{\partial u^+}{\partial r^+}\right|_{r^+=\xi R^+ -0} = \frac{\beta}{Da^{1/2}R^+}u_i^+ \tag{39}$$

where u_i^+ is the dimensionless filtration velocity at the interface, and β is the dimensionless adjustable coefficient [35,36].

Substituting Eq. (38) into Eq. (39) results in:

$$\left(\frac{\nu_{\text{eff}}/\nu_f}{1+\nu_T^+|_{\xi R^+}}\right)\left.\frac{\partial u^+}{\partial r^+}\right|_{\xi R^+ +0} + \frac{1}{1+\nu_T^+|_{\xi R^+}} = \frac{\beta}{Da^{1/2}R^+}u_i^+ \tag{40}$$

Eq. (40) gives the second boundary condition (in addition to Eq. (35)) necessary for the determination of the velocity profile in the porous region by solving Eq. (23).

In addition to Eq. (40), continuity of the filtration velocity, temperature, and heat flux is imposed at the interface, at $r^+ = \xi R^+$. This translates into the following hydrodynamic boundary condition:

$$u^+|_{r^+=\xi R^+-0} = u^+|_{r^+=\xi R^+ +0} = u_i^+ \tag{41}$$

the following thermal boundary conditions for the *uniform wall heat flux case*:

$$\theta|_{r^+=\xi R^+-0} = \theta|_{r^+=\xi R^+ +0},\qquad \left.\frac{\partial\theta}{\partial r^+}\right|_{r^+=\xi R^+-0} = \frac{k_{\text{eff}}}{k_f}\left.\frac{\partial\theta}{\partial r^+}\right|_{r^+=\xi R^+ +0} \tag{42}$$

and the following thermal boundary conditions for the *uniform wall temperature case*:

$$\phi|_{r^+=\xi R^+-0} = \phi|_{r^+=\xi R^+ +0},\qquad \left.\frac{\partial\phi}{\partial r^+}\right|_{r^+=\xi R^+-0} = \frac{k_{\text{eff}}}{k_f}\left.\frac{\partial\phi}{\partial r^+}\right|_{r^+=\xi R^+ +0} \tag{43}$$

respectively.

In the center of the duct, $r^+ = 0$, for the *uniform wall heat flux case* the following symmetry condition is imposed:

$$\frac{\partial\theta}{\partial r^+} = 0 \tag{44}$$

For the *uniform wall temperature case* the appropriate boundary condition at $r^+ = 0$ is:

$$\frac{\partial\phi}{\partial r^+} = 0 \tag{45}$$

No hydrodynamic boundary condition is needed in the center of the duct because Eq. (1) is a first-order equation; the required boundary condition for Eq. (1) is given by Eq. (41) once the filtration velocity on the porous side of the interface is found by solving Eq. (23) with boundary conditions given by Eqs. (35) and (40).

3. Results and discussion

Dimensionless governing equations are discretized by a finite-difference method leading to algebraic systems of equations with tridiagonal matrices. Nonlinearities in these equations are handled by Gauss–Siedel iterations. Convergence of iterations is improved, when necessary, by using the relaxation technique. Parameter values utilized in the computations (unless a different value is explicitly shown on the figure) are summarized in Table 1.

It should be noted that Re_p is not an independent parameter; its value can be deduced from definitions of Re_p and R^+ and Eq. (17) as:

$$Re_p = R^+\frac{\sqrt{180}(1-\varphi)}{\varphi^{3/2}}Da^{1/2} \tag{46}$$

The major assumption made in this research is that the flow in the clear fluid region is turbulent while the flow in the porous region is laminar. To prove that this assumption is valid it is necessary to estimate Reynolds numbers in the clear fluid and porous regions and compare them with their critical values.

As shown in [20], the Reynolds number based on the width of the clear fluid region, $2\xi R$, and the mean velocity in this region, $(U_m)_{\text{clear }fl}$, is defined as:

$$Re_{2\xi R} = (U_m)_{\text{clear }fl}2\xi R/\nu_f = \left(U_m^+\right)_{\text{clear }fl}2\xi R^+ \tag{47}$$

Table 1
Parameter values utilized in computations

c_F	C	k_m/k_f	Pr	Pr_t	R^+	β	μ_{eff}/μ_f	ξ	φ
0.55	0.1	1	1	1	10^3	0	1	0.7	0.95

where $(U_m^+)_{\text{clear } fl}$ is the dimensionless mean velocity in the clear fluid region, $(U_m)_{\text{clear } fl}/u_\tau$:

$$\left(U_m^+\right)_{\text{clear } fl} = \frac{2}{(\xi R^+)^2} \int_0^{\xi R^+} u^+ r^+ \, \mathrm{d}r^+ \tag{48}$$

For the flow in a duct, the critical Reynolds number is 4×10^3.

For the porous region, the Reynolds number based on $K^{1/2}$ is defined as:

$$Re_K = v_{\text{fil}} K^{1/2}/\nu_f \tag{49}$$

where K is the permeability of the porous medium.

For small values of the Darcy number, the velocity profile in the porous region consists of three regions [37], two boundary layers (one adjacent to the solid wall and the other adjacent to the porous/fluid interface) and a constant velocity region between them. In this constant velocity region, the second term on the left-hand side of Eq. (23) is negligible, and the velocity can be obtained by solving a simple quadratic equation as:

$$u_{\text{bulk}}^+ = -\frac{1}{2c_F Da^{1/2} R^+} + \left[\left(\frac{1}{2c_F Da^{1/2} R^+}\right)^2 + \frac{2Da^{1/2}}{c_F \xi}\right]^{1/2} \tag{50}$$

Estimating filtration velocity, v_{fil}, in the bulk of the fluid region as $v_{\text{fil}} = u_\tau u_{\text{bulk}}^+$, Eq. (49) can be recast as:

$$Re_K = R^+ Da^{1/2} \left\{ -\frac{1}{2c_F Da^{1/2} R^+} + \left[\left(\frac{1}{2c_F Da^{1/2} R^+}\right)^2 + \frac{2Da^{1/2}}{c_F \xi}\right]^{1/2} \right\} \tag{51}$$

According to Bear [23], most experiments indicate that actual turbulence in porous media occurs at values of the Reynolds number at least one order of magnitude higher than the Reynolds number at which deviation from the Darcy law is observed due to the Forchheimer (quadratic drag) effects. According to Nield and Bejan [29], transition from Darcy to Forchheimer flow regime occurs when Re_K is larger than 10. This means that the turbulent flow regime may occur in porous media if Re_K is larger than 100.

Computational results for $c_F = 0.55$, $R^+ = 10^3$, $\beta = 0$, $\mu_{\text{eff}}/\mu_f = 1$, and $\xi = 0.7$ are given in Table 2. It can be seen that for all values of the Darcy number utilized in these computations the value of $Re_{2\xi R}$ is much larger than

Table 2
Reynolds numbers in the clear fluid and porous regions of the channel

Da	$Re_{2\xi R}$	Re_K
0.00001	18 515	0.08
0.0001	20 011	1.54
0.001	22 063	11.94
0.01	25 033	71.17

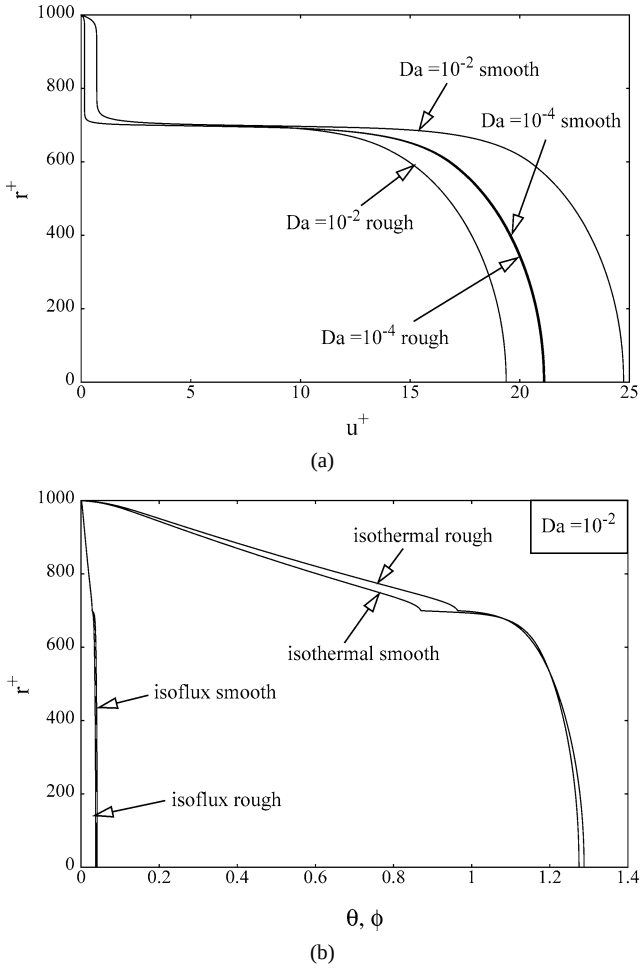

Fig. 2. Distributions of dimensionless velocity (a) and dimensionless temperature (b) in the duct.

the critical Reynolds number of 4×10^3. This indicates that the flow in the clear fluid region is turbulent. At the same time, Re_K is much smaller than 100. This means that the assumption of the flow in the clear fluid region being turbulent and in the porous region being laminar is a reasonable one. Again, as follows from [24], the model suggested in this research may be valid even if the flow in the porous region is in transition to turbulence or even weakly turbulent.

Fig. 2(a) displays velocity distributions in the duct computed for two values of the Darcy number, $Da = 10^{-2}$ and $Da = 10^{-4}$, assuming either rough or hydraulically smooth interface. For the case of $Da = 10^{-2}$, the velocity profiles that correspond to the rough and smooth interfaces, respectively, are remarkably different; results for the rough interface case predict significantly smaller velocity in the clear fluid region. This is because in the case of a rough interface, the eddy viscosity in the clear fluid region is much larger than in the case of a hydraulically smooth interface. The case of $Da = 10^{-4}$, however, exhibits almost no difference between velocity profiles for the rough and smooth interfaces. This is because, in accordance with Eq. (18), the

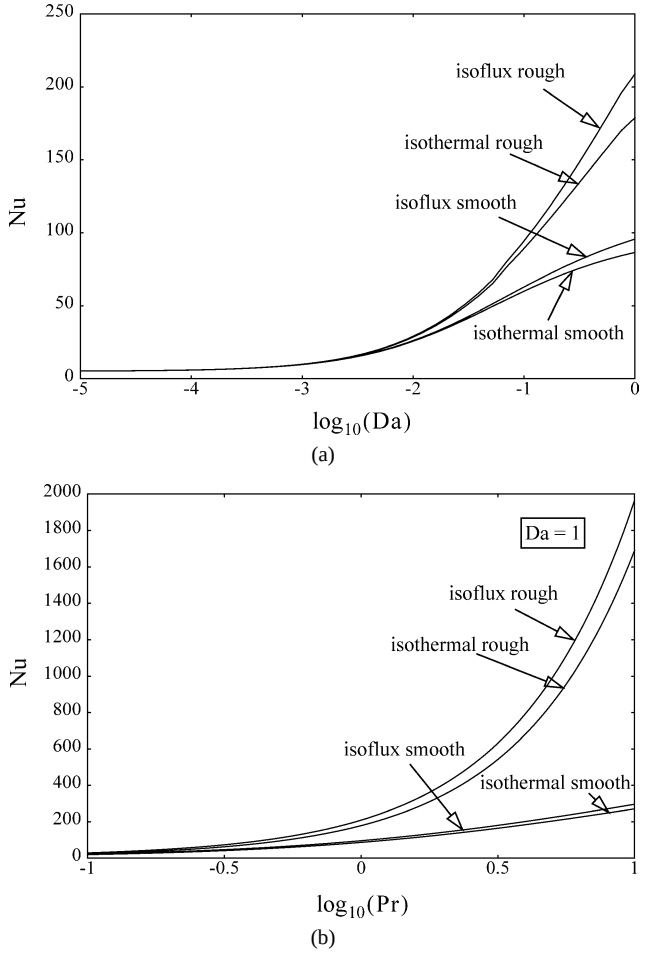

Fig. 3. Effect of the Darcy number on the Nusselt number (a) and effect of the Prandtl number on the Nusselt number (b).

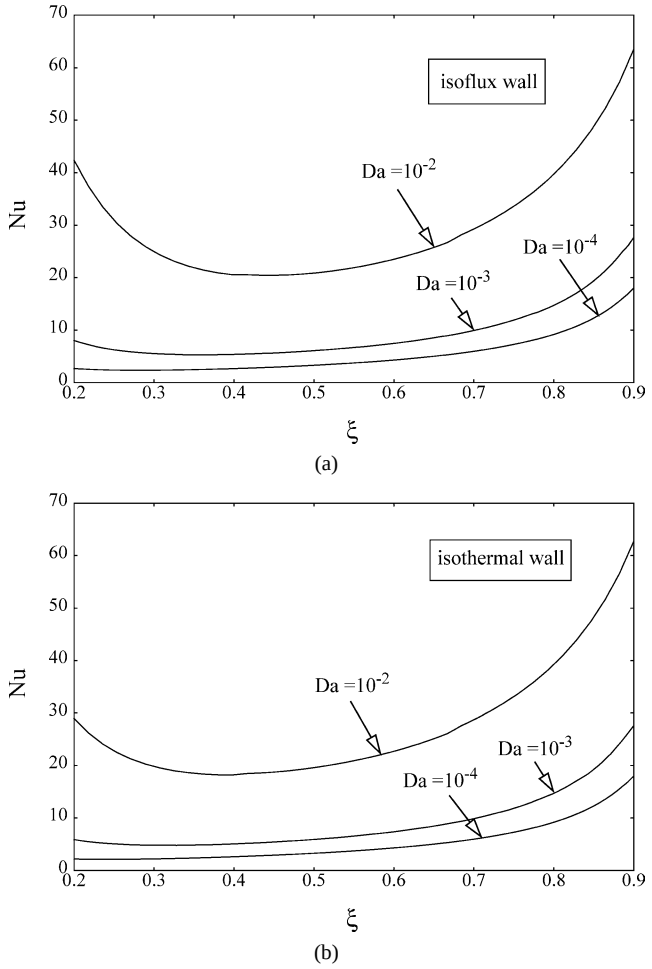

Fig. 4. Effect of position of the porous/fluid interface on the Nusselt number for uniform wall heat flux (a) and uniform wall temperature (b).

equivalent sand-grain roughness of the interface is proportional to the square root of the Darcy number. This means that the equivalent sand-grain roughness of the interface for $Da = 10^{-4}$ is ten times smaller than that for $Da = 10^{-2}$. It should be noted that the accuracy of the assumption that the flow in the porous layer can be modeled as laminar degrades when increasing the Darcy number. Therefore, model predictions for a large Darcy number are less accurate than for a small Darcy number; however, the conclusion about the significant effect the interface roughness on turbulent flows in composite porous/fluid domains is not restricted by the validity of a particular turbulence model utilized in this research.

Fig. 2(b) displays the dimensionless temperature distributions obtained for $Da = 10^{-2}$ for both uniform wall heat flux and uniform wall temperature cases, computed assuming either rough or hydraulically smooth interface. The large difference between the curves for the uniform wall heat flux and uniform wall temperature cases is explained by different definitions of the dimensionless temperature for these two cases (see Eqs. (26) and (30), respectively).

Fig. 3(a) displays the effect of the Darcy number on the Nusselt number for both uniform wall heat flux and uniform wall temperature cases. It can be seen that the Nusselt number computed with the rough interface assumption is larger than that computed with the smooth interface assumption, and that the deviation between the rough and smooth values of the Nusselt number increases as the Darcy number increases. This is because equivalent sand-grain roughness of the interface is proportional to the square root of the Darcy number, as follows from Eq. (18).

Fig. 3(b) displays the effect of the Prandtl number on the Nusselt number. These computations are carried out for $Da = 1$ assuming that the turbulent Prandtl number, Pr_t, remains equal to unity for any value of Pr. The effect of the Prandtl number is to increase the Nusselt number.

Figs. 4(a) and (b) display the effect of position of the porous/fluid interface on the Nusselt number for uniform wall heat flux and uniform wall temperature, respectively. According to Fig. 1, a larger value of ξ corresponds to a larger clear fluid region and a thinner porous layer at the duct wall. Computations are not carried out all the way up to $\xi = 0$ (that would corresponds to a duct completely filled with a porous medium) because it would be incorrect to utilize the model developed in this paper for computing turbulent flow

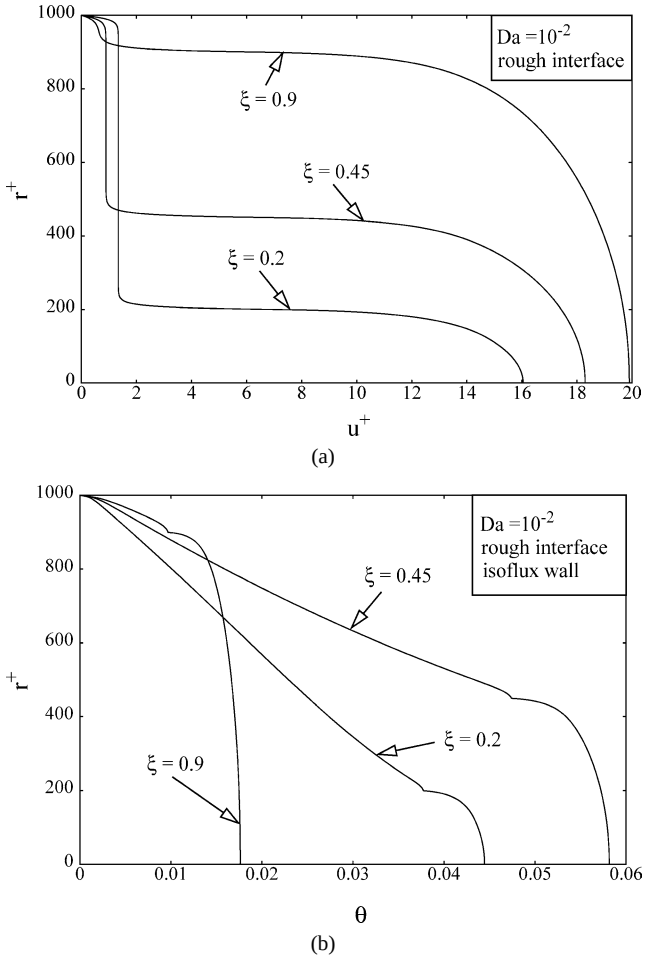

Fig. 5. Distributions of dimensionless velocity (a) and dimensionless temperature (b) in the duct for the uniform wall heat flux case, $Da = 10^{-2}$, for three values of ξ: 0.2, 0.45, and 0.9.

in porous media. The model relies on the assumption that there is a sufficiently large clear fluid region which carries most of the flow. If the clear fluid region vanishes (as it happens when $\xi \to 0$), the flow is forced to go through the porous region, which may result in the transition to turbulence in the porous region. The increase of the Nusselt number, which is observed with the increase of ξ for $\xi > 0.5$, is expected. Indeed, the porous region acts as an insulating layer and the decrease of the thickness of this layer should result in an increase of the Nusselt number. The unexpected feature in Figs. 4(a) and (b) is that the Nusselt number takes on its minimum value somewhere between $0.2 \leqslant \xi \leqslant 0.5$, depending on the value of the Darcy number (the larger is *Da*, the larger is the value of ξ at which minimum of the Nusselt number occurs). The minimum is observed for both uniform wall heat flux and uniform wall temperature cases.

To explain the unexpended increase of the Nusselt number with a decrease of ξ, Figs. 5(a) and (b) display dimensionless velocity and temperature profiles, respectively, computed for the uniform wall heat flux case for $Da = 10^{-2}$. According to Fig. 4(a), for these parameters the minimum value of the Nusselt number occurs at $\xi = 0.45$. Figs. 5(a) and (b) display dimensionless velocity and temperature profiles for three values of ξ, namely, 0.2, 0.45, and 0.9. According to Fig. 5(a), a decrease of ξ leads to an increase of velocity in the porous region, near the duct wall. This is because as the clear fluid opening in the center of the duct closes, more fluid is forced to go through the porous region. An increase of velocity near the wall leads to an increase of the curvature of the temperature profile near the wall, which has the effect of flattening the overall temperature profile (compare curves in Fig. 5(b) that correspond to $\xi = 0.45$ and $\xi = 0.2$, respectively). This leads to a decrease in the magnitude of $T_m - T_W$, which in turn leads to an increase in the magnitude of *Nu* as ξ becomes smaller.

A jump in the temperature derivative at the porous/fluid interface in Fig. 5(b) is caused by the difference of fluid thermal conductivity (molecular plus turbulent) and effective thermal conductivity of the porous medium (which is composed of a stagnant thermal conductivity and thermal conductivity due to thermal dispersion).

4. Conclusions

A model that enables computing turbulent flow in composite porous fluid/domains is developed. To account for the roughness of the porous/fluid interface turbulent flow in the clear fluid region is computed utilizing a combined two-layer κ–l and κ–ε model. It is found that the dependence of the Nusselt number on the position of the interface exhibits a minimum for both uniform wall heat flux and uniform wall temperature cases.

Acknowledgements

The author gratefully acknowledges NSF grant # CTS-0226021 and grant # NAG3-2706 awarded to him by NASA Office of Biological and Physical Research, Physical Sciences Division.

References

[1] B.V. Antohe, J.L. Lage, A general two-equation macroscopic model for incompressible flow in porous media, Internat. J. Heat Mass Transfer 40 (1997) 3013–3024.
[2] D. Getachew, W.J. Minkowycz, J.L. Lage, A modified form of the κ–ε model for turbulent flows of an incompressible fluid in porous media, Internat. J. Heat Mass Transfer 43 (2000) 2909–2915.
[3] K.Y. Chung, K.S. Lee, W.S. Kim, Modified macroscopic turbulence modeling for the tube with channel geometry in porous media, Numer. Heat Transfer A 43 (2003) 659–668.
[4] M.J.S. de Lemos, M.H.J. Pedras, Recent mathematical models for turbulent flow in saturated rigid porous media, ASME J. Fluids Engrg. 123 (2001) 935–940.
[5] M.H.J. Pedras, M.J.S. de Lemos, On the mathematical description and simulation of turbulent flow in a porous medium formed by an array of elliptic rods, ASME J. Fluids Engrg. 123 (2001) 941–947.

[6] M.H.J. Pedras, M.J.S. de Lemos, Macroscopic turbulence modeling for incompressible flow through undeformable porous media, Internat. J. Heat Mass Transfer 44 (2001) 1081–1093.
[7] M.H.J. Pedras, M.J.S. de Lemos, Simulation of turbulent flow in porous media using a spatially periodic array and a low *Re* two-equation closure, Numer. Heat Transfer A 39 (2001) 35–59.
[8] M.H.J. Pedras, M.J.S. de Lemos, On the definition of turbulent kinetic energy for flow in porous media, Internat. Comm. Heat Mass Transfer 27 (2000) 211–220.
[9] T. Masuoka, Y. Takatsu, T. Inoue, Chaotic behavior and transition to turbulence in porous media, Microscale Thermophys. Engrg. 6 (2002) 347–357.
[10] D.W. Barr, Turbulent flow through porous media, Ground Water 39 (2001) 646–650.
[11] G. Alvarez, P.E. Bournet, D. Flick, Two-dimensional simulation of turbulent flow and heat transfer through stacked spheres, Internat. J. Heat Mass Transfer 46 (2003) 2459–2469.
[12] D. Flick, A. Leslous, G. Alvarez, Semi-empirical modeling of turbulent fluid flow and heat transfer in porous media, Internat. J. Refrig. 26 (2003) 349–359.
[13] P. Vadasz, Small and moderate Prandtl number convection in a porous layer heated from below, Internat. J. Energy Res. 27 (2003) 941–960.
[14] J.L. Lage, The fundamental theory of flow through permeable media from Darcy to turbulence, in: D.B. Ingham, I. Pop (Eds.), Transport Phenomena in Porous Media, Elsevier, Oxford, 1998, pp. 1–30.
[15] S. Hahn, J. Je, H. Choi, Direct numerical simulation of turbulent flow with permeable walls, J. Fluid Mech. 450 (2002) 259–285.
[16] M. Prakash, O.F. Turan, Y.G. Li, J. Mahoney, G.R. Thorpe, Impinging round jet studies in a cylindrical enclosure with and without a porous layer: Part I—Flow visualizations and simulations, Chem. Engrg. Sci. 56 (2001) 3855–3878.
[17] M. Prakash, O.F. Turan, Y.G. Li, J. Mahoney, G.R. Thorpe, Impinging round jet studies in a cylindrical enclosure with and without a porous layer: Part II—LDV measurements and simulations, Chem. Engrg. Sci. 56 (2001) 3879–3892.
[18] R.A. Silva, M.J.S. de Lemos, Turbulent flow in a channel occupied by a porous layer considering the stress jump at the interface, Internat. J. Heat Mass Transfer 46 (2003) 5113–5121.
[19] M.J.S. de Lemos, R.A. Silva, Turbulent flow around a wavy interface between a porous medium and a clear domain, in: Proceedings of the ASME FEDSM '03, 4th ASME/JSME Joint Fluids Engineering Conference, Honolulu, Hawaii, USA, July 6–11, 2003, ASME, New York, 2003, ASME paper FESM2003-45457.
[20] A.V. Kuznetsov, M. Xiong, Development of an engineering approach to computations of turbulent flows in composite porous/fluid domains, Internat. J. Thermal Sci. 42 (2003) 913–919.
[21] T. Masuoka, Y. Takatsu, Turbulence model for flow through porous media, Internat. J. Heat Mass Transfer 39 (1996) 2803–2809.
[22] D.A. Nield, Turbulence model for flow through porous media—Comments, Internat. J. Heat Mass Transfer 40 (1997) 2499.
[23] J. Bear, Dynamics of Fluids in Porous Media, Elsevier, New York, 1972 (corrected reprint, Dover, New York, 1988).
[24] H.H. Macedo, U.M.S. Costa, M.P. Almeida, Turbulent effects on fluid flow through disordered porous media, Physica A 299 (2001) 371–377.
[25] P.A. Durbin, G. Medic, J.-M. Seo, J.K. Eaton, S. Song, Rough wall modification of two-layer k–ε, ASME J. Fluids Engrg. 123 (2001) 16–21.
[26] W. Rodi, Experience with two-layer models combining the k–ε model with a one-equation model near the wall, in: Proceedings of the 29th Aerospace Sciences Meeting, Reno, Nevada, January 7–10, 1991, pp. 1–12, AIAA-91-0216.
[27] D.C. Wilcox, Turbulence Modeling for CFD, DCW Industries, La Canada, CA, 1994.
[28] T. Cebeci, K.C. Chang, Calculation of incompressible rough-wall boundary-layer flows, AIAA J. 16 (1978) 730–735.
[29] D.A. Nield, A. Bejan, Convection in Porous Media, second ed., Springer, New York, 1999.
[30] D.A. Nield, Private communication, 2003.
[31] A. Amiri, K. Vafai, Transient analysis of incompressible flow through a packed bed, Internat. J. Heat Mass Transfer 41 (1998) 4259–4279.
[32] A. Amiri, K. Vafai, Analysis of dispersion effects and non-thermal equilibrium, non-Darcian, variable porosity incompressible flow through porous media, Internat. J. Heat Mass Transfer 37 (1994) 939–954.
[33] O.A. Plumb, The effect of thermal dispersion on heat transfer in packed bed boundary layers, Proc. ASME JSME Thermal Engrg. Joint Conf. 2 (1983) 17–22.
[34] A. Bejan, Heat Transfer, Wiley, New York, 1993.
[35] J.A. Ochoa-Tapia, S. Whitaker, Momentum transfer at the boundary between a porous medium and a homogeneous fluid—I. Theoretical development, Internat. J. Heat Mass Transfer 38 (1995) 2635–2646.
[36] J.A. Ochoa-Tapia, S. Whitaker, Momentum transfer at the boundary between a porous medium and a homogeneous fluid—II. Comparison with experiment, Internat. J. Heat Mass Transfer 38 (1995) 2647–2655.
[37] A.V. Kuznetsov, Analytical study of fluid flow and heat transfer during forced convection in a composite channel partly filled with a Brinkman–Forchheimer porous medium, Flow Turbulence Combust. 60 (1998) 173–192.